Controlling Salt Damage | 2011-02

Princeton University

National Park Service
U.S. Department of the Interior

National Center for Preservation Technology and Training

Final Report: Controlling Salt Damage November 1, 2010

Grant Number: MT-2210-09-NC-03

Principal investigator: George W. Scherer

Contact information:

Prof. George W. Scherer
Princeton University
Dept. Civil & Env. Eng/PRISM
Eng. Quad. E-319
Princeton, NJ 08544 USA

Phone:	1-609-258-5680
FAX:	1-609-258-1563
Email:	scherer@princeton.edu
URL:	http://web.me.com/gwscherer1/SchererGroup

Project team:

Prof. George W. Scherer (PI)
Dr. Rosa Espinosa (Post-doctoral researcher, now at ETH, Zurich)
Ms. Meg McNall (Graduate student, Dept. Civil & Env. Eng., Princeton)
Mr. Ararimeh Aiyejima (Undergraduate, graduated June, 2009)

Table of Contents

Executive Summary	2
Introduction	3
Materials	8
Methods	8
Results and Discussion	10
Conclusions	
Publications	
References	

Executive Summary:

Growth of salt crystals within the pores of stone can cause serious damage. Salt may enter with ground water or be created by reaction of the minerals in the stone with atmospheric pollutants. As water evaporates from the pores of the stone, the salt concentration rises and the crystals grow until they approach the pore walls. If the salt came into direct contact with the stone, then growth would stop and there would be no stress. However, in most cases there is a repulsive force between the salt and mineral surfaces, so that they do not touch; instead, the salt remains surrounded by film of solution that encourages it to grow and exert pressure on the pore walls. The goal of this study was to develop a chemical treatment for limestone that would eliminate the repulsion, and thereby prevent salt from applying pressure on the pore walls. On the basis of screening tests, the polymer chosen for testing was polyacrylic acid with low molecular weight (~5000). Potassium hydroxide is used to raise the pH of the polymer solution to 7-8, and the solution is equilibrated with calcium carbonate before being introduced into the stone, where the polymer adsorbs on the pore walls. When crystals of sodium sulfate are induced to grow within the stone, the damage is strongly reduced by the coating in most cases. To date, there are problems of reproducibility with the treatment that are not fully understood. Possible explanations are discussed and additional research directions are proposed.

Introduction.

One of the most obvious manifestations of the stress exerted by crystals growing in confined spaces is the damage done by salt in a remarkable range of environments, from seashores to cities to deserts [1], attacking the modern infrastructure as well as ancient monuments. Despite the ubiquity and seriousness of the problem, the details of the mechanism by which a growing crystal generates stress and cracking are incompletely understood. As a result, remedies to retard deterioration are based on empirical approaches and have proven, in some instances, to accelerate damage. In contrast, strategies grounded in a better fundamental understanding of the salt/water/pore wall interface, show promise of mitigating, or even eliminating, damage. The goal of the present work is to improve our understanding of the mechanisms by which salts cause damage to porous materials, and to develop a procedure for treating stone to protect against such damage. The work specifically involves use of a polymeric film to reduce the interfacial energy between salt and minerals surfaces, an idea originally suggested by the PI [2], which has shown considerable promise in preliminary experiments [3]. The immediate goal of the work is to evaluate the durability of this type of treatment, to test it against a variety of relevant salts, and to optimize the application of the treatment so that field tests can be initiated (in a subsequent study).

Observations by earlier workers, discussed in ref. 4, indicate that when a crystal grows within the pores of a stone there is a liquid film between the salt crystal and the pore wall [5,6,7,8], which implies that a repulsive (disjoining) force exists between the surfaces [9]. In the case of ice crystals, it can be shown [4] that the van der Waals interaction is repulsive, owing to the unusual circumstance that liquid water is denser than solid ice; this means that the Hamaker constant of the water lies between that of the ice and the mineral, resulting in repulsive forces [10]. However, in the case of salts, the crystal should be attracted to the wall by van der Waals forces, so the repulsion must have some other origin. In a DOE-sponsored project, we are performing molecular dynamics simulation of the salt/solution/mineral interfacial region to identify the nature of this repulsion. Results to date indicate that the dominant forces are electrostatic effects related to the distribution of dissolved ions and the orientation of the water dipoles [11], which is consistent with the conclusions of other experimental and theoretical studies [12, 13]. As long as the liquid film exists between the crystal and the mineral surface, the

crystal is in contact with a supersaturated solution, so it attempts to grow and exerts pressure on the pore wall. By eliminating this liquid film, and replacing it with a dry, low-energy interface, the adsorbed polymeric layer would eliminate this stress.

Salts in stone become concentrated owing to evaporation of the water or a change in temperature, and crystals may grow if supersaturation occurs. If a crystal nucleates in a supersaturated solution, its growth can be stopped by applying a pressure, p, to its surface. The magnitude of the required pressure is [9,14,15]

$$p = \left(\frac{R_g T}{V_m} \right) \ln \left(\frac{K}{K_0} \right) \tag{1}$$

where R_g is the gas constant, T is the absolute temperature, V_m is the molar volume of the crystal, and K and K_0 are the solubility products of the supersaturated and saturated solutions, respectively. It is the pore walls that must exert the pressure to prevent the growth of a crystal within a porous body. As explained in detail in ref. 4, tens of megapascals may be required to stop the growth in the presence of a modest supersaturation. Only part of the pressure in Eq. (1) is supplied by the pore wall; the rest is related to the surface energy and curvature of the crystal. When conditions of thermodynamic equilibrium prevail, the pressure on the wall is greatest in small pores in the presence of a high supersaturation [4,16]. In fact, it is unusual for stones to have pores small enough (< 100 nm) to generate high stresses, under equilibrium conditions. On the other hand, nonequilibrium conditions result during evaporation of pore liquid, when the solution retreats into the gap between an existing salt crystal and the pore wall, as shown in Figure 1. In that case, very high stresses can be generated by large crystals, because the supersaturation can only be reduced by growing toward the wall. This may be the primary mechanism by which salt does damage in the field [17, 18].

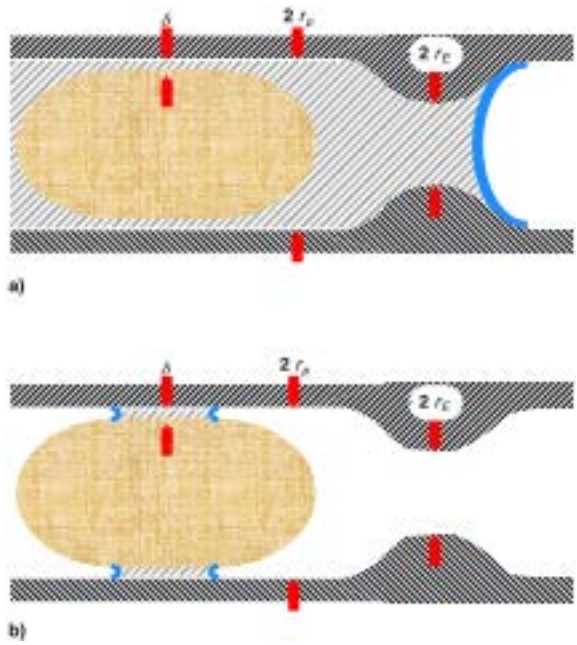

Figure 1. a) Crystal in a large pore cannot generate high stresses at equilibrium, but (b) when evaporation has driven the liquid into the gap (width δ) between the crystal and the pore wall, the sides of the crystal are no longer in equilibrium and the stress is controlled only by the supersaturation and the interfacial repulsion. From ref. 18.

Thus, in large or small pores, it is the repulsive pressure between the salt and the pore wall that sets the upper bound on the stress that can be exerted. In either case, the damage can be avoided by eliminating the repulsion, so that the salt crystal comes into contact with the pore wall and stops growing. For example, if limestone is saturated with an aqueous solution of polyacrylic acid (neutralized with KOH), the polymer binds to the pore wall, because the deprotonated carboxyl groups bind to the calcium ions of the calcium carbonate crystal. Binding is expected to occur at a few sites along the polymer chain, leaving loops of the polymer chain free to interact with any salt crystals that approach the pore wall. As the salt crystal binds to the polymer, it stops growing and the development of pressure is avoided. The favorable interaction of sodium sulfate with calcite surfaces coated with PAA was demonstrated in ref. 3. The effectiveness of the treatment is demonstrated in Figure 2. The sample on the left is bare limestone, and it was destroyed within about one week of exposure to capillary rise of a 12 wt% solution of Na_2SO_4. The amount of PAA applied to the stone increases from left to right, and the two samples on the right (with coatings of PAA estimated to be 8-10 nm thick) are clearly much

less damaged. In the present work, we studied whether the treatment is durable (that is, whether it desorbs), and what the optimal amount is for a given limestone.

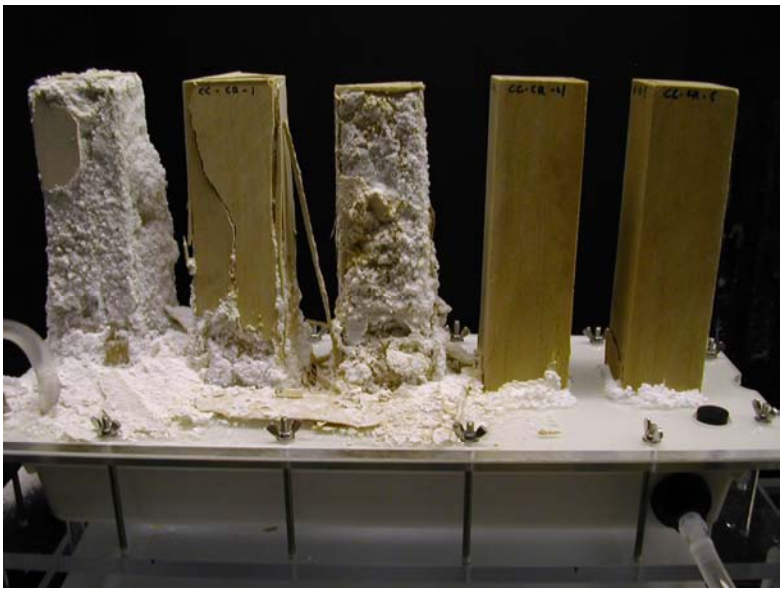

Figure 2. This photo shows 5 samples of Cordova Cream limestone treated with amounts of PAA increasing from zero at the left to a layer about 10 nm thick at the right. The stones are standing in a bath of sodium sulfate, and were exposed to 39% RH for about 5 weeks.

A more quantitative measure of the effectiveness of the treatment is the warping test, in which a plate of stone is impregnated with sodium sulfate (by immersing in a solution and then drying), then glued to a plate of glass. When water wicks into the stone, it dissolves the anhydrate (thenardite), which creates a solution that is supersaturated with respect to the decahydrate ($Na_2SO_4 \cdot 10H_2O$, mirabilite) [19, 20]. The growth of mirabilite generates a high crystallization pressure that makes the stone expand; since it is attached to a non-expanding plate of glass, the bilayer warps, and the deflection is a measure of the pressure exerted by the salt in the pores. The results of such a test are illustrated in Figure 3, where the stress in the stone has been calculated from the measured deflection. If the limestone plate is untreated, the deflections are large and the stone is damaged, but if the stone was pretreated with PAA, the deflections are small and no damage is visible.

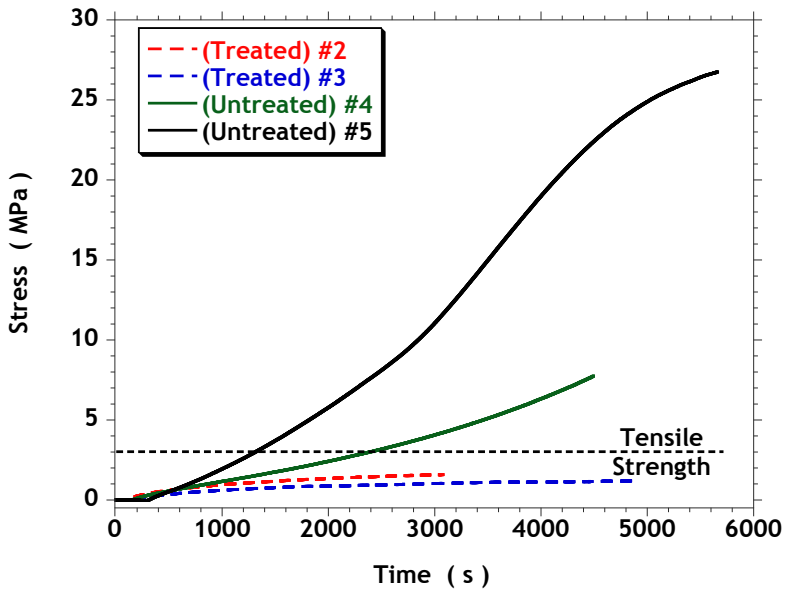

Figure 3. Stress in Cordova Cream limestone from crystallization of sodium sulfate; stress calculate from deflection of bilayer composite consisting of stone and glass plates joined with epoxy. Bare stone (Untreated) experiences stress higher than the measured tensile strength (~3 MPa), whereas the stress in stone pretreated with PAA is not high enough to cause failure.

In the preliminary warping tests, the stress in the treated stones reached about half of the tensile strength, and subsequent measurements of the elastic modulus of the stone showed a decrease of about 10%. Therefore, the performance of the treatment, while quite impressive, could certainly be improved. Moreover, the design of the test can be improved by reducing the amount of salt, so that no damage occurs; in that case, the stress from crystallization can be accurately found from an elastic analysis of the deflection of the sample. Extensive evaluation of this test has shown that it permits quantitative evaluation of the crystallization pressure from the salt [21]; however, it was also demonstrated that the distribution of the salt in the stone is nonuniform, so the mathematical analysis is complicated. For that reason, we have abandoned that test in favor of dilatometry.

We have recently published reviews, partially supported by the present grant, describing the state of the art in salt crystallization theory and the experimental methods that are being used to improve our understanding of the underlying physics [22, 23].

Materials.

Tests were performed on several limestones. Indiana limestone is a gray oolitic carbonate rock, mainly composed of calcite (> 97.3 wt%), and a small amount of other components, such as Al_2O_3, SiO_2 and $MgCO_3$ [24]. It consists mainly of calcite-cemented oolites, but a small amount of sparry calcite crystals may be also present. Cordova Cream limestone (also known as Austin chalk) contains calcareous microorganisms composed of clear calcite set in a structureless matrix of microcrystalline calcite, and it is a lightly bedded [25]. Cadeby Stone is a light cream-colored stone classified as dolo-oomicrite with dolomite as major component and small amounts of other components, such as iron oxides, calcite and barium sulfates. The MIP data [26] of this stone show a pore size distribution between 0.1 and 10 μm, and a total porosity measured by vacuum impregnation ~21.5 vol%. The amount of pores smaller than 0.1 μm is negligible, while 89% of the porosity is formed by pores in the range from 0.1 to 5 μm. The sorptivity of this stone is 0.064 ± 0.02 cm/min$^{1/2}$ and the capillary water uptake 15.7 vol%. Highmoor stone is a dolo-microsparite white magnesian limestone consisting of fine dolomite crystals in micritic cements. Patches of dark iron oxide can be observed in thin sections. This stone has spherical pores and a homogeneous structure. The MIP data [26] show a unimodal pore size distribution. The total porosity measured by vacuum impregnation is around 24.6 ± 1.4%, 47% of the pores being larger than 5 μm. The amount of pores smaller than 0.1 lm is negligible. The sorptivity of the stone is 0.055 ± 0.02 cm/min$^{1/2}$ and the capillary water uptake 11.8 vol%.

Polyacrylic acid with a molecular weight of 5000 was obtained in the form of a 50 wt% aqueous solution (Polysciences Inc).

Methods.

Thermogravimetric analysis (TGA) was used to assess the adsorption of PAA on calcite samples. Pure calcite powder and PAA solutions were run in a Perkin Elmer TGA 7 (using nitrogen purge gas) as controls. To determine the concentration of PAA (wt%) in the control solutions, samples were heated in the TGA to 110 °C to drive off water and held at that temperature until they reached constant weight. The percent of sample weight remaining at this point was then taken as the concentration by weight of PAA in the control solutions.

For determination of adsorbed PAA with different concentrations of bulk solution, samples of 250 mg of calcite powder were equilibrated with 10 ml of PAA solutions of varying concentrations by mixing with a magnetic stirrer for several hours. Solutions of both pH ~3.5 (pH of the PAA solutions) and of alkaline pH (obtained by addition of solid KOH) were used. The calcite was separated from the solution by vacuum filtration, so that both the filtrate and recovered powder could be analyzed via TGA. The stable weight at 110°C was taken as the initial weight for calcite samples, and the stable weight at ~325°C was taken as the weight after PAA had been decomposed [27]. At higher temperatures, the pure calcite lost weight, but powdered calcite exposed to a KOH solution showed no significant weight lost at ≤ 350˚C, so that temperature was the highest used for these tests.

To evaluate how readily the PAA layer would be removed by the movement of water through the pores of a stone, washout experiments were performed. A 40 mg sample of the PAA-treated calcite samples from each PAA-calcite mixture was stirred with 5 ml of deionized water or calcite solution for 3 days, prior to thermogravimetric analysis.

It was observed that the pH of the PAA-calcite solutions changed over time, which could indicate a continuous change in the surface of the calcite and its zeta potential. To minimize this effect, we explored the effect of adjusting the pH of PAA solutions to different levels with KOH before mixing with calcite. One gram of calcite powder was continuously stirred with 40 ml deionized water or 0.2% PAA solutions adjusted to pH of 3.6 (no KOH added), 7.2, 8.2 and 9.2 using KOH, and the pH of each solution was checked over time. The 0.2% PAA solution was representative of the range of concentrations under investigation, within which a monolayer was expected.

Capillary rise tests were performed using the apparatus shown in Figure 2**. The equipment is explained in more detail in ref. 18. The relevant properties of the stone are shown in Table 1**

Table 1. The last column is the concentration of PAA that would be expected to produce an adsorbed monolayer (~5 nm) or a fractional layer (1 nm) on the pore walls, as explained below. PAA solutions were prepared at concentrations 0.5, 0.75, 1.0, and 1.5 wt%, and the pH was adjusted to neutral using KOH. The solution was allowed to wick into samples of each stone with approximate dimensions of 5 x 5 x 25 cm. Once saturated, the samples were allowed to dry under ambient conditions, then placed into contact with a bath of 12 wt% sodium sulfate (as in Figure 2). The first test used two sets of stones: five samples of the Cadeby limestone and five of

the Indiana limestone. Each set contained an untreated stone, as well as stones treated with neutralized PAA solutions at concentrations of 0.5, 0.75, 1.0, and 1.5 wt%. The test was run on ten samples of Cordova Cream limestone, using the treatment levels from the previous test.

To measure the density of the polymer solution as a function of its concentration, 15 solutions were made containing between 0.05 and 20 weight percent PAA. Each of these solutions was then analyzed using a Paar density meter with an accuracy of three decimal places.

Table 1. Properties of stone used in capillary rise test

Stone	Porosity	Density (g/cm^3)	S[1] (cm^2/g)	c_T (wt%) [2]			
				δ = 1 nm	5 nm	1 nm	5 nm
				ρ_P = 1.3 g/cm^3		1.0 g/cm^3	
Cordova Cream	0.239	2.05	11,688	1.3	6.4	1.0	5.0
Indiana	0.139	2.31	4,961	1.1	5.3	0.83	4.1
Highmoor	0.251	2.08	5,100	0.55	2.7	0.42	2.1
Cadeby	0.181	2.17	8,900	1.4	6.8	1.1	5.3

[1] Surface area by BET method, using nitrogen as adsorbate

[2] c_T = concentration of solution required to produce adsorbed layer with thickness δ, assuming that the density of the adsorbed layer is ρ_P

Results and Discussion.

When the calcite powder is exposed to the polymer solution, the pH changes with time, as shown in Figure 4. The pH stabilizes at a value between 8.3 and 9, depending on the concentration of KOH in the solution. Rapid equilibration is achieved at pH 7.2, and attack on the calcite at that pH is minimal, so this is the pH range used in the testing the salt resistance of the PAA treatment.

As shown in Figure 5, the amount of PAA adsorbed on calcite increases almost linearly with the concentration of the polymer solution up to about 0.19%, after which the amount adsorbed remains nearly constant. Increasing the concentration by an order of magnitude causes only a slight additional deposit, as shown in Figure 6. This is about 5 times the concentration

found to produce monolayer coverage in the study by Thompson et al. [28], but their polymers were not neutralized; moreover, as explained below, we apparently obtained multilayer coverage.

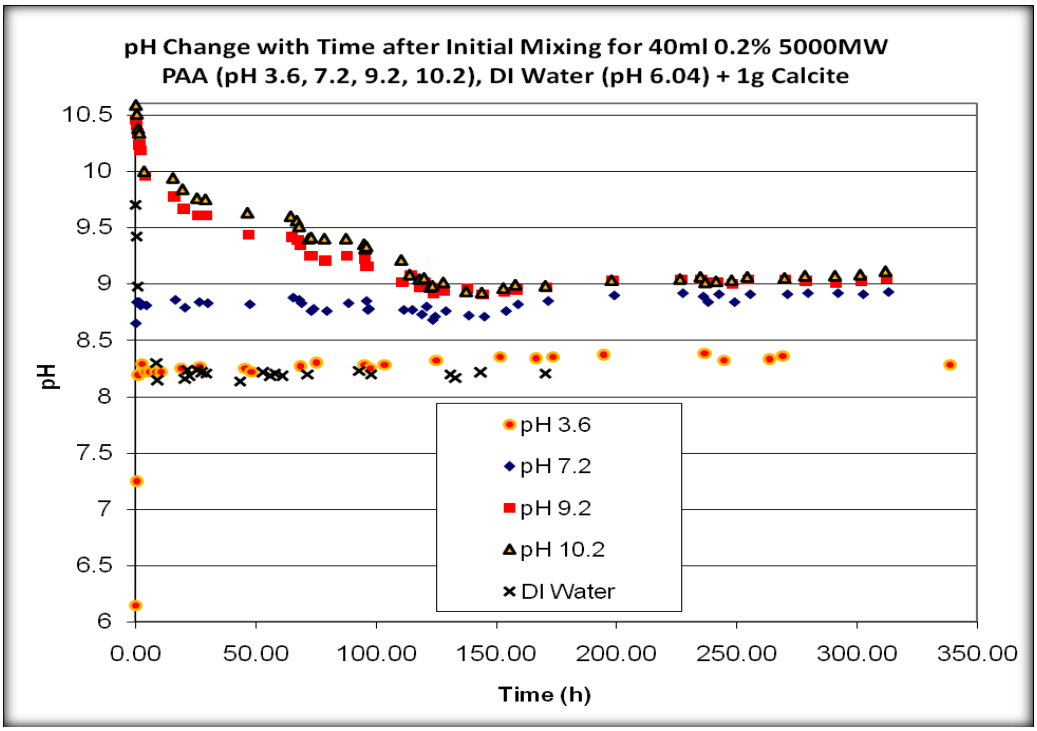

Figure 4. Time dependence of pH for mixtures of calcite powder with PAA solutions of different pH (adjusted by addition of KOH)

The adsorption measurements were made on a calcite powder with specific surface area $S_{BET} = 4465$ cm^2/g. The weight percent adsorbed, c_A , is

$$c_A = \frac{100\, m_P}{m_C + m_P} \tag{2}$$

where m_P is the mass of polymer adsorbed on mass m_C of calcite, whose total surface area is $S = m_C\, S_{BET}$. The mass of adsorbed polymer per unit area of calcite is

$$m_A = \frac{m_P}{S} = \frac{c_A}{(100 - c_A) S_{BET}} \tag{3}$$

where the second equality follows from eq. (2).

The adsorption data can be fitted to a Langmuir isotherm of the form

$$m_A = \frac{m_A^{\max} K c_S}{1 + K c_S} \tag{4}$$

where m_A is the mass adsorbed per unit area in equilibrium with a solution containing concentration c_S of polymer, and K is a constant. From the fit in Figure 6, we find that K = 8.36 and the maximum amount of polymer that can be adsorbed is $m_A^{\max}$ = 0.058 m^2/g = 5.8 x 10^{-6} cm^2/g.

If ρ_P is the density of the adsorbed layer of polymer, then the layer thickness of adsorbed polymer, δ, is

$$\delta = \frac{m_A}{\rho_P} = \left(\frac{m_A^{\max}}{\rho_P}\right)\frac{K c_S}{1 + K c_S} \tag{5}$$

With ρ_P in g/cm^3 and c_S in weight percent, the adsorbed thickness in nanometers is

$$\delta\ (\mathrm{nm}) = \left(\frac{485}{\rho_P}\right)\frac{c_S}{1 + 8.36\, c_S} \tag{6}$$

The density ρ_P to be used in eq. (5) depends on the configuration of the adsorbed polymer. We do not know that value, but it is certainly bounded by the density of the solid polymer, $\rho_P^{\max}$ = 1.3 g/cm^3 [29], and the density of the solvent, $\rho_P^{\min}$ = 1.0 g/cm^3, which would be approached if the polymer were highly dilated. These two bounds are used for the calculations in Table 1. At the peak of adsorption, where $m_A = m_A^{\max}$, eq. (5) indicates that δ lies between about 45 and 58 nm for the maximum and minimum adsorbed densities, respectively.

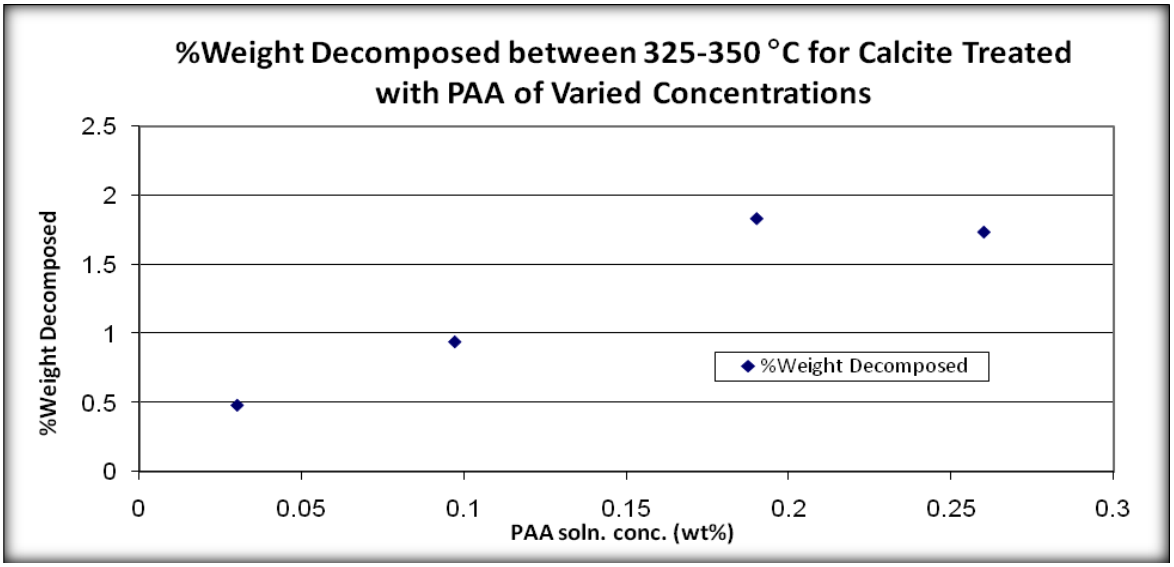

Figure 5. Relationship between the amount of PAA adsorbed onto calcite and concentration of PAA solution used to treat calcite, deetermined by wt% of treated calcite samples decomposed at temperatures between 325 and 350°C. Average of values of multiple runs used where possible.

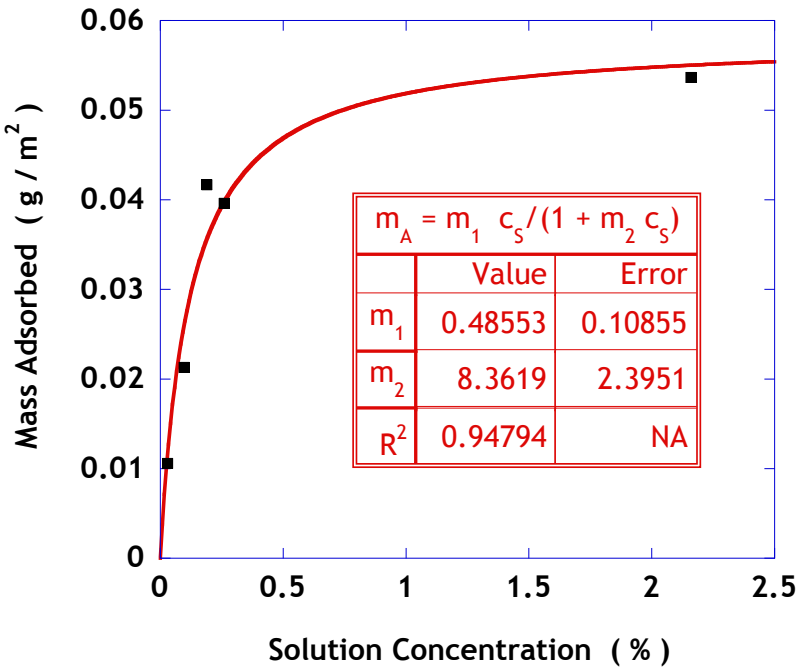

Figure 6. Relationship between the amount of PAA adsorbed onto calcite and concentration of solution up to 2.16% PAA. Data fit to eq. (4).

The radius of gyration of a PAA molecule with a molecular weight of 5000 is estimated to be about $r_G \approx 2.6$ nm, based on the data of Reith et al. [30]. Estimating the thickness of an adsorbed monolayer to be $\delta_M \approx 2r_G \approx 5$ nm [31], we conclude that our peak adsorption was about 10 monolayers thick. The deprotonated polymer layers may have been bound together by calcium ions liberated from the calcite substrate, as well as potassium ions from the KOH used to neutralize the solution. In practice, we do not want that much polymer to adsorb, because desorption of those layers would result in free PAA that could act as a nucleation inhibitor for salt. That could be dangerous: if the salt concentration in the pores built to the point that the inhibitor was consumed, then the supersaturation could be so large that the crystals would grow with extremely high chemical potential. For that reason, we want only enough polymer to constitute ≤ 1 monolayer.

To achieve monolayer coverage, we want to choose c_S such that $\delta \leq \delta_M$. According to eq. (5), this means that the solution in equilibrium with the adsorbed layer should have a concentration of $c_M \approx 0.011$-0.015 wt% (estimated using $\rho_P^{\min}$ and $\rho_P^{\max}$, respectively). Of course, this applies in the case where there is an infinite reservoir of solution at that concentration. In contrast, during treatment of stone, the volume of the solution is limited to the volume of the pores. Our goal is to introduce a solution into the stone such that the concentration drops to c_M *after* the monolayer of polymer has adsorbed.

Suppose that the stone has pore volume V_p (cm^3/g) = ϕ/ρ_B , porosity ϕ, bulk density ρ_B, and specific surface area S (cm^2/g). When the stone is saturated, in every gram of stone there is a volume of solution equal to V_p in contact with surface area S, onto which it deposits thickness δ of polymer with density ρ_P. The mass of the adsorbed polymer per gram of stone is $M_A = S\,\delta\,\rho_P$. The specific volume of solution remaining after equilibration is $V_S = V_p - S\,\delta$, and it is intended to contain concentration $c_\infty = c_M$. The concentration (wt%) of polymer remaining in solution per gram of stone is found from

$$c_\infty = \frac{100\,M_S}{V_S\,\rho_S[c_\infty] + M_S} \tag{7}$$

where $\rho_S[c_\infty]$ is the density of a solution with concentration c_∞. The initial concentration (mass fraction) of the solution used for the treatment is given by

$$c_T = \frac{100\left(M_A + M_S\right)}{\left(V_p - \left(M_A + M_S\right)/\rho_P\right)\rho_S[c_T] + M_A + M_S} \tag{8}$$

The density of the solution as a function of PAA concentration, shown in Figure 7, is approximated by

$$\rho_S\left(\mathrm{g/cm^3}\right) = 0.999 + 0.302\, c_S\left(\mathrm{wt\%}\right) \tag{9}$$

We are interested in relatively dilute solutions, so we can approximate ρ_S by ρ_W, the density of water. Therefore, the concentration of the treatment is

$$c_T = \frac{100\left[\left(100 - c_\infty\right) S\,\delta\,\rho_P^2 + c_\infty\left(V_p - S\,\delta\right)\rho_P\,\rho_w\right]}{V_p\,\rho_w\left(100\,\rho_P - c_\infty\,\rho_w\right) + S\,\delta\left(\rho_P - \rho_w\right)\left[\left(100 - c_\infty\right)\rho_P - c_\infty\,\rho_w\right]} \tag{10}$$

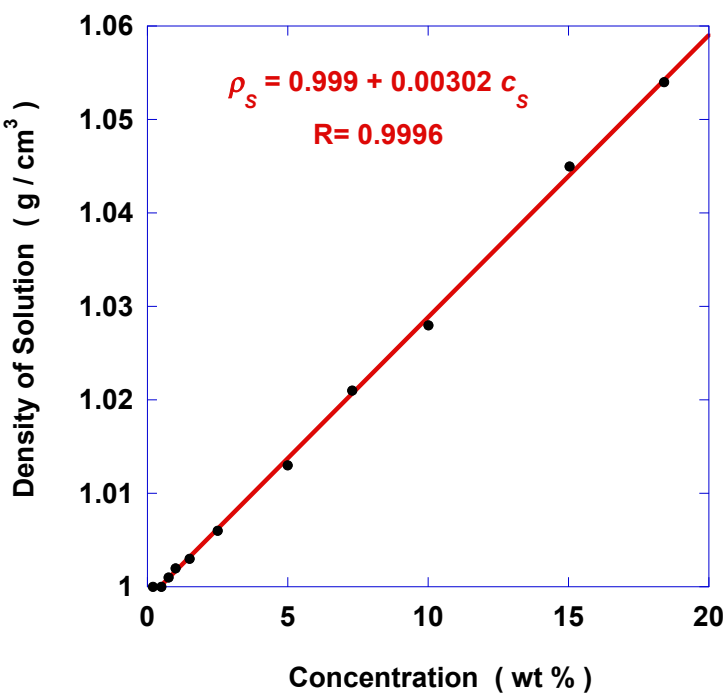

Figure 7. Density of solution of PAA (molecular weight 2000) versus concentration.

Since the target final concentration is $c_\infty \approx 0$, this reduces to

$$c_T \approx \frac{100 S \delta \rho_P}{V_p \rho_w + S\delta(\rho_P - \rho_w)} \approx \frac{100 S \delta \rho_P}{\phi \rho_w / \rho_B + S\delta(\rho_P - \rho_w)} \tag{11}$$

This formula differs insignificantly from the exact solution, based on eqs. (8) and (9), which used to calculate the concentrations shown in the last column of Table 1.

Based on these results, PAA solutions were prepared at concentrations of 0.5, 0.75, 1.0, and 1.5 wt%. The predicted thickness of the layer deposited by these solutions is shown in Table 2, for polymer densities of $\rho_P^{\min}$ and $\rho_P^{\max}$. These submonolayer levels were chosen with the intention of minimizing free polymer in the pore solution.

Table 2. Predicted thickness δ (nm) of deposited PAA layer inside stone in capillary rise tests

ρ_P (g/cm^3) =	1.0				1.3			
c_T (wt%) =	0.50	0.75	1.0	1.5	0.50	0.75	1.0	1.5
Stone								
Cordova Cream	0.50	0.75	0.99	1.5	0.38	0.57	0.77	1.2
Indiana	0.60	0.91	1.2	1.8	0.47	0.70	0.93	1.4
Highmoor	1.2	1.8	2.4	3.5	0.91	1.4	1.8	2.7
Cadeby	0.47	0.70	0.94	1.4	0.36	0.54	0.72	1.1

In the first capillary rise test, the Cadeby and Indiana limestones behaved similarly. The untreated samples were the first to show signs of damage, followed by the heavily (1.5 wt%) and lightly (0.5 wt%) treated samples. In the case of the heavily treated samples, the damage originated deeper inside the stone than in the lightly treated and untreated samples. For both sets of stone, the moderately (0.75 and 1.0 wt %) treated samples lasted the longest, suggesting that the adsorbed layers provided protection against crystallization pressure without excessive desorption. The earlier failure of the more heavily treated stone (estimated to have about 1/3 of a monolayer adsorbed) suggests that some of the polymer has desorbed and inhibited precipitation, leading eventually to growth at higher supersaturations. If significant desorption occurs from a partial layer, then this treatment will be too difficult to control for field use. On the other hand, it may be that the treatments were too conservative: if submonolayers provide insufficient

protection, then significant crystallization stresses would have developed in the stone, in which case the damage reflects random variations in sample strength, rather than a meaningful pattern. The latter interpretation is supported by the second capillary rise test, in which 10 samples of Cordova Cream were tested with a similar range of layer thickness, and the results showed no discernible pattern. Future tests will explore a wider range of PAA concentration.

Conclusions.

Use of polyacrylic acid shows promise for protection of limestone against crystallization pressure, but the treatment has not yet been brought under control. In the capillary rise tests, inconsistent results were obtained, which might reflect an excessively conservative application of polymer. Future tests will explore a wider range of compositions. To provide quantitative information, dilatometric tests will be performed on samples of stone during crystallization [32] to determine the effect of PAA treatment on the stress generated in the stone.

Publications related to this work:

"Crystallization of sodium sulfate salts in limestone", R.M. Espinosa-Marzal, G.W. Scherer, Env. Geo. 56 [3-4] (2008) 605-621

"Study of the pore clogging induced by salt crystallization in Indiana limestone", R. M. Espinosa Marzal, G. W. Scherer, Proc. 11th Int. Cong. Deterioration and Con-servation of Stone (Nicolaus Copernicus University Press, Torun, Poland, 2008) Vol. I, pp. 81-88

"Mechanisms of damage by salt", R.M. Espinosa-Marzal & G. W. Scherer, pp. 61-77 in Limestone in the Built Environment: Present-Day Challenges for the Preservation of the Past. B.J. Smith, M. Gomez-Heras, H.A. Viles & J. Cassar (eds), Special Publications 331 (Geological Society, London, 2010)

"Advances in Understanding Damage by Salt Crystallization", R.M. Espinosa-Marzal & G. W. Scherer, Accounts of Chemical Research 43 [6] (2010) 897-905

References.

---

1. A. Goudie and H. Viles, *Salt Weathering Hazards*, (Wiley, Chichester, 1997) 241 pp.

2. G.W. Scherer, R. Flatt, and G. Wheeler, "Materials Science Research for Conservation of Sculpture and Monuments", MRS Bulletin, Jan. 2001, pp. 44-50

3. J. Houck and G.W. Scherer, "Controlling stress from salt crystallization", pp. 299-312 in Fracture and Failure of Natural Building Stones, ed. S.K. Kourkoulis (Springer, Dordrecht, 2006)

4. G.W. Scherer, "Crystallization in pores", Cement Concr. Res. 29 [8] (1999) 1347-1358; "Reply to discussion of Crystallization in pores", G.W. Scherer, Cement and Concr. Res. 30 [4] (2000) 673-675

5. J. Lavalle, "Recherches sur la formation lente des cristaux à la température ordinaire" (Research on the slow formation of crystals at ordinary temperature), Compte Rend. Acad. Sci. (Paris) 36 (1853) 493-495

6. G.F. Becker and A.L. Day, "Note on the linear force of growing crystals", J. Geology XXIV [4] (1916) 313-333

7. S. Taber, "The growth of crystals under external pressure", Am. J. Sci. 41 (1916) 532-556

8. A.E. Corte, "Vertical migration of particles in front of a moving freezing plane", J. Geophys. Res., 67 [3] (1962) 1085-1090

9. C.W. Correns, "Growth and dissolution of crystals under linear pressure", Disc. Faraday Soc. 5 (1949) 267-271

10. J. Israelachvili, *Intermolecular & Surface Forces*, 2nd ed. (Academic, London, 1992)

11. M. Webb, S. Garofalini, and G.W. Scherer, research supported by DOE grant DEFG02-97ER45642, to be published

12. S. Veeramasuneni, Y. Hu, M.R. Yalamanchili, and J.D. Miller, "Interaction Forces at High Ionic Strengths: The Role of Polar Interfacial Interactions", J. Colloid Interface Sci. 188 (1997) 473–480

13. S. Veeramasuneni, M.R. Yalamanchili, j. D. Miller, "Interactions between dissimilar surfaces in high ionic strength solutions as determined by atomic force microscopy", Colloids and Surfaces A: Physicochemical and Engineering Aspects 131 (1998) 77-87

14. R.J. Flatt, M. Steiger, G.W. Scherer, “A commented translation of the paper by C.W. Correns and W. Steinborn on crystallization pressure”, Env. Geo. 52 [2] (2007) 187-203

15. M. Steiger, "Crystal growth in porous materials—I: The crystallization pressure of large crystals", Journal of Crystal Growth 282 (2005) 455–469

16. D.H. Everett, "The thermodynamics of frost damage to porous solids", Trans. Faraday Soc., 57 (1961) 1541-1551

17. G.W. Scherer, “Stress from crystallization of salt in pores”, in *Proc. 9th Int. Cong. Deterioration and Conservation of Stone*, Vol. 1, ed. V. Fassina (Elsevier, Amsterdam, 2000) p. 187

18. G.W. Scherer, “Stress from crystallization of salt”, Cement Concr. Res. 34 (2004) 1613-1624

19. S. Chatterji and A.D. Jensen, "Efflorescence and breakdown of building materials", Nordic Concrete Res. 8 (1989) 56-61

20. R.J. Flatt, "Salt damage in porous materials: how high supersaturations are generated", J. Cryst. Growth 242 (2002) 435-454

21. R.M. Espinosa-Marzal, A. Hamilton, M. McNall, K. Whitaker, and G.W. Scherer, “The chemomechanics of sodium sulfate crystallization in thenardite impregnated limestones during re-wetting”, submitted to J. Materials Research

22. R.M. Espinosa-Marzal & G. W. Scherer, “Mechanisms of damage by salt”, pp. 61-77 in Limestone in the Built Environment: Present-Day Challenges for the Preservation of the Past. B.J. Smith, M. Gomez-Heras, H.A. Viles & J. Cassar (eds), Special Publications 331 (Geological Society, London, 2010)

23. R.M. Espinosa-Marzal & G. W. Scherer, “Advances in Understanding Damage by Salt Crystallization”, Accounts of Chemical Research 43 [6] (2010) 897-905

24. T. Perry, N. M. Smith, W. J. Wayne, “Salem limestone and associated formations in south-central Indiana”. Field Conference Guidebook 7 (Indiana Department of Conservation, Geological Survey, 1954)

25. B. Haimson, “Micromechanisms of borehole instability leading to breakouts in rocks”, Int. J. Rock Mechanics and Mining Sciences 44 (2007) 157-173

26. A. Bourgès, “Holistic correlation of physical and mechanical properties of selected natural stones for assessing durability and weathering in the natural environment”. Dissertation, Ludwigs-Maximilians-Universität München (2006)

27. M.A. Moharram, M.G. Khafagi, “Thermal Behavior of Poly(acrylic acid)-Poly(vinyl pyrrolidone) and Poly(acrylic acid)-Metal-Poly(vinyl pyrrolidone) Complexes”, J. Appl. Polym. Sci. 102 (2006) 4049-4057

28. M. Thompson, S.J. Wilkins, R.G. Compton, and H.A. Viles, "Polymer coatings to passivate calcite from acid attack: polyacrylic acid and polyacrylonitrile", J. Colloid Interface Sci. 260 (2003) 204–210

29. A.B. Argade and N.A. Peppas, "Poly(acrylic acid)–Poly(vinyl alcohol) Copolymers with Superabsorbent Properties", Journal of Applied Polymer Science, 70(1998) 817–829

30. D. Reith, B. Müller, F. Müller-Plathe, and S. Wiegand, "How does the chain extension of poly (acrylic acid) scale in aqueous solution? A combined study with light scattering and computer simulation", J. Chem. Phys. 116 (2002) 9100-9106

31. P.G. de Gennes, "Polymers at an interface: A simplified view", Adv. Colloid Interface Sci. 27 (1987) 189-209

32. R.M. Espinosa-Marzal, G.W. Scherer, “Crystallization of sodium sulfate salts in limestone”, Env. Geo. 56 [3-4] (2008) 605-621